Structural and Dielectric Properties Hexaferrite/Poly (Vinyl Alcohol) Composites

Amrin Kagdi, Rajshree B. Jotania*

Department of Physics, University School of Sciences, Gujarat University,
Ahmedabad 380 009, India

Abstract

Magnetic barium cobalt hexaferrite particles-PVA composites with of different mass ratio: 9:1, 8:2, 7:3, 6:4 and 5:5 were prepared. Structural properties of the composites were characterized by Infrared spectroscopy (FTIR), X-ray diffraction (XRD) and scanning electron microscope (SEM). The effect of the concentration of $Ba_2Co_2Fe_{28}O_{46}$ hexaferrites on structural and dielectric properties of magnetic-PVA composites were investigated. FTIR result revealed that composite samples show absorption peaks of both ferrites and PVA. The X-ray diffraction investigations confirm the formation of mono phase of hexaferrite particles. Scanning electron microscopy images reveal that the shape and size of barium cobalt hexaferrite powder particles is irregular. The addition of PVA not much changed the shape and size of particles (ranging from 200-300 nm) but porosity found to decrease.

Keywords: barium cobalt hexaferrites, PVA, XRD, SEM, dielectric properties

*Author for Correspondence E-mail:rbjotania@gmail.com

INTRODUCTION

Hexaferrites are found to be a technologically important class of magnetic oxides and widely used as permanent magnet material in household products such as refrigerator, magnetic recording media, microwave absorbers because they have high Curie temperature, high saturation magnetization, high electrical resistivity, low eddy current and dielectric loss, excellent chemical stability, corrosion resistance and they are relatively cheap to produce. The crystal structure of X-type hexaferrites (Figure 1) is closely related to M and W- type and constructed as stack of hexagonal R-block and spinel S-block along the hexagonal c-axis with a model as RSR*S*S*(the '*' indicates the rotation of corresponding block by 180 ° around the c-axis) [1, 2]. The chemical formula of X-type hexaferrite is 2 $BaO\cdot2$ $MeO\cdot14$ Fe_2O_3; (where Me represents 3d-transition metal element). Braun [3] reported the crystal structure of $Ba_2Fe_{30}O_{46}$ hexaferrite. The crystallographic and magnetic characteristics of the metallic sublattices in the X-type $BaMe_2Fe_{28}O_{46}$ hexaferrite is shown in Table 1.

Table 1: *The Crystallographic and Magnetic Characteristics of the Metallic Sublattices in the X-type $BaMe_2Fe_{28}O_{46}$ Hexaferrite.*

Block	Coordination	Number per block	Expected spin direction
R	Octahedral	2	Down
R	Trigonalbipyramidal	1	Up
R-S	Octahedral	3	Up
S	Octahedral	1	Up
S	Tetrahedral	2	Down
S-S	Octahedral	3	Up

Although there have been many investigations into ferrite powder–polymer composites but less work reported on ferrite-polymer composites where PVA is chosen as matrix [4–6]. Crystallographic x-ray diffraction and magnetic data of polycrystalline samples of

_____

X-type hexagonal ferrites reported by Gu et al. [7–9]. G. Xiong and Mai [10] reported preparation and magnetic properties of that $Ba_2Co_2Fe_{28}O_{46}$ (Co$_2$X) nanocrystals. Pullar and Bhattacharya [11] studied synthesis and characterization of stoichiometric Co$_2$X fibers were prepared using a sol-gel based process.

The preparation and microwave properties of $Ba_2Zn_xCo_{2-x}Fe_{28}O_{46}$ hexaferrites reported by Haijun et al. [12,13]. Crystallographic and magnetic properties of Cu$_2$X, Co$_2$X, and Ni$_2$X hexaferrites published by Kenji Kamishima et al. [14] Strontium based X-type ferrite $Sr_2Fe_{30}O_{46}$ is also reported [15].
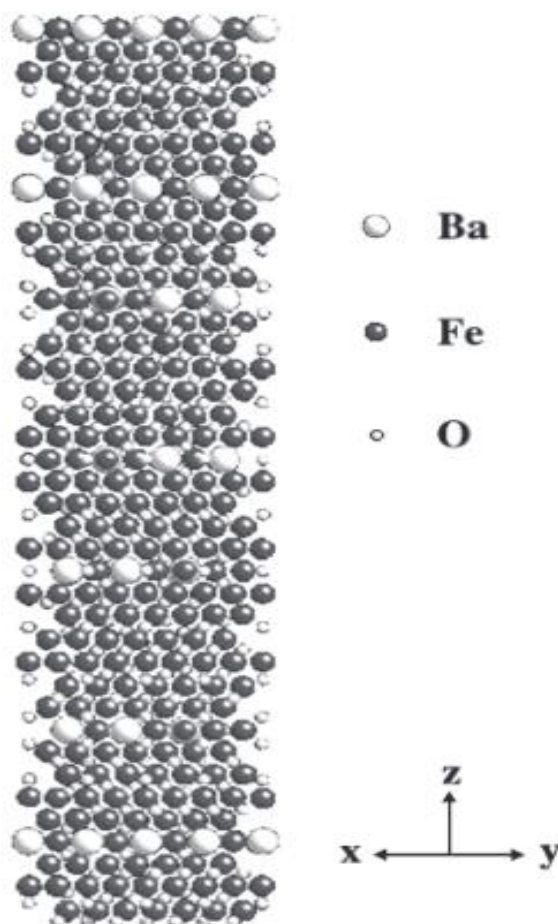

Fig. 1: Crystal Structure of X-type Hexaferrite [3].

PVA; -[-CH2-CHOH-]n-) is a white, odorless, water-soluble, semi-crystalline synthetic polymer. PVA has a two dimensional hydrogen-bonded network sheet structure and widely used in diverse applications such as adhesives for paper, wood, textiles, leather, other water-absorbent, surgical devices, sutures, hybrid islet transplantation, implantation, blend membrane and in synthetic cartilage in reconstructive joint surgery [16-19]. The X-type hexaferrite with chemical composition $Ba_2Co_2Fe_{28}O_{46}$ chosen for this study. The $Ba_2Co_2Fe_{28}O_{46}$ hexaferrite powder was prepared using a reverse co-precipitation technique. The $Ba_2Co_2Fe_{28}O_{46}$ hexaferrite powder (filler) –

PVA (matrix) composite samples were prepared by mixing ferrite powder to gather with PVA in different mass ratio 9:1, 8:2, 7:3, 6:4 and 5:5. The mixed powder pressed in a steel mould under 55 MPa for 300 s. In present paper we report structural and dielectric properties of $Ba_2Co_2Fe_{28}O_{46}$ hexaferrite (filler)–PVA (matrix) composites.

MATERIALS AND METHODS
The reverse co-precipitation technique is used to X-type $Ba_2Co_2Fe_{28}O_{46}$ hexaferrite powder. The Ba(No$_3$)$_2$, Co(No$_3$)$_2$, Fe(No$_3$)$_3$ dissolved in distilled water according to weight formula, then sodium hydroxide was added drop until the precipitates form (pH~7). The obtained

_____

solution kept 24 hours for aging and then filtered. The radish precursors recollected and kept at 100 °C for 24 h then grind well. The dried powder preheated at 450 °C for 4 h in a muffle furnace and finally material is sintered at 950°C for 4 h to obtain barium-cobalt hexaferrite powder. The $Ba_2Co_2Fe_{28}O_{46}$ hexa ferrite mixed well with PVA (poly vinyl alcohol) in different mass ratio 9:1, 8:2, 7:3, 6:4 and 5:5 to prepare $Ba_2Co_2Fe_{28}O_{46}$–PVA composites. The structural properties of the composites were characterized by Infrared spectroscopy (FTIR), X-ray diffraction (XRD) and scanning electron microscope (SEM). The
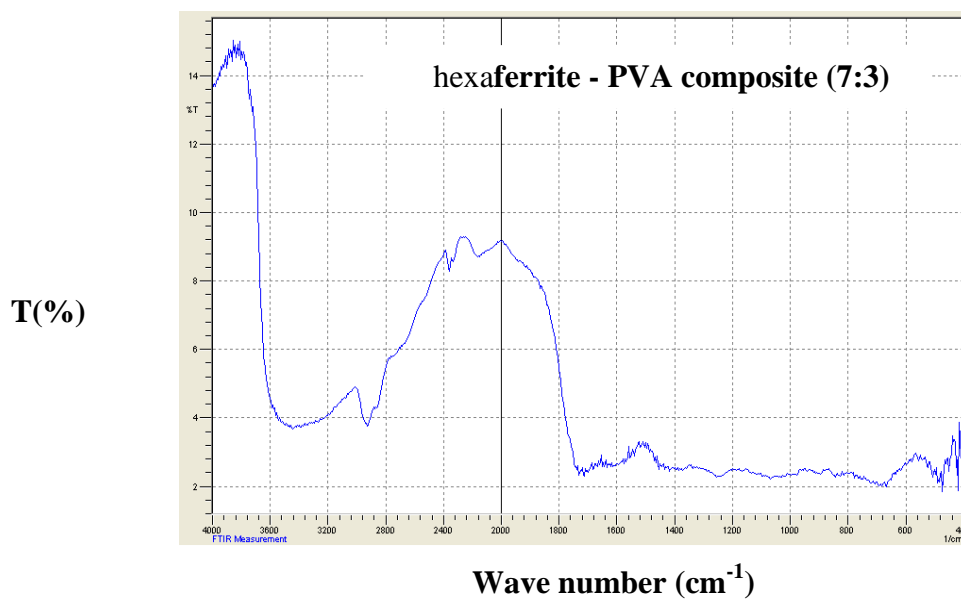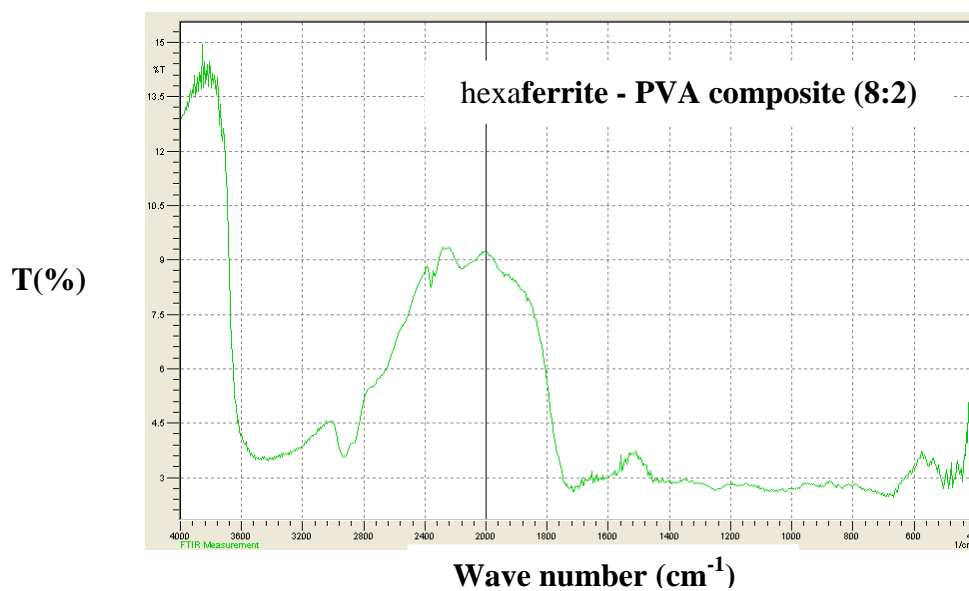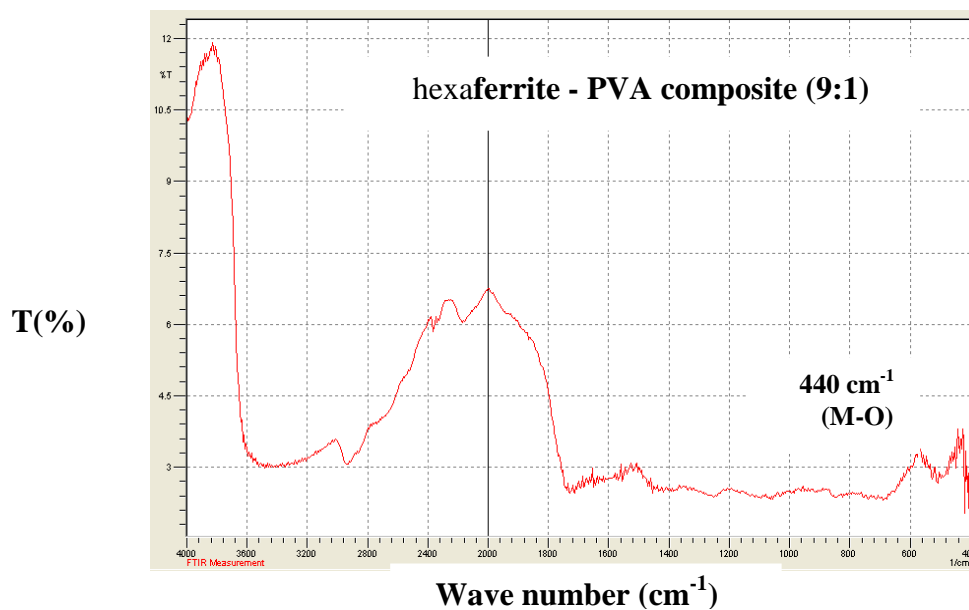
effect of the concentration of $Ba_2Co_2Fe_{28}O_{46}$ hexaferrites on structural and dielectric properties of magnetic-PVA composites was investigated.

RESULTS AND DISCUSSION
FTIR analysis
FTIR spectra of ferrite, PVA and composite samples were obtained within the range between 4,000 cm^{-1} and 400 cm^{-1} using FTIR spectrometer (Bruker Tensor 27 Model).
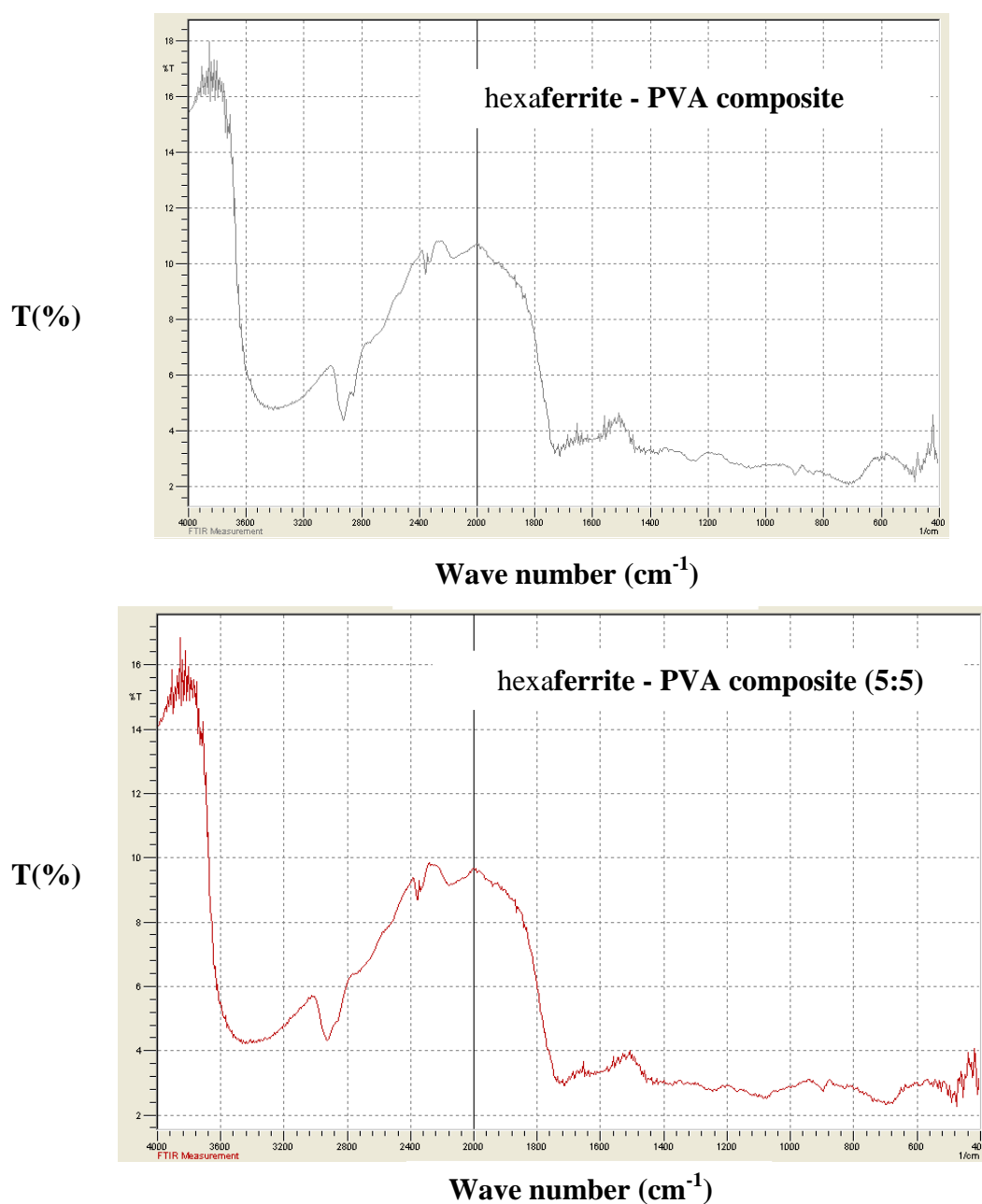
_____
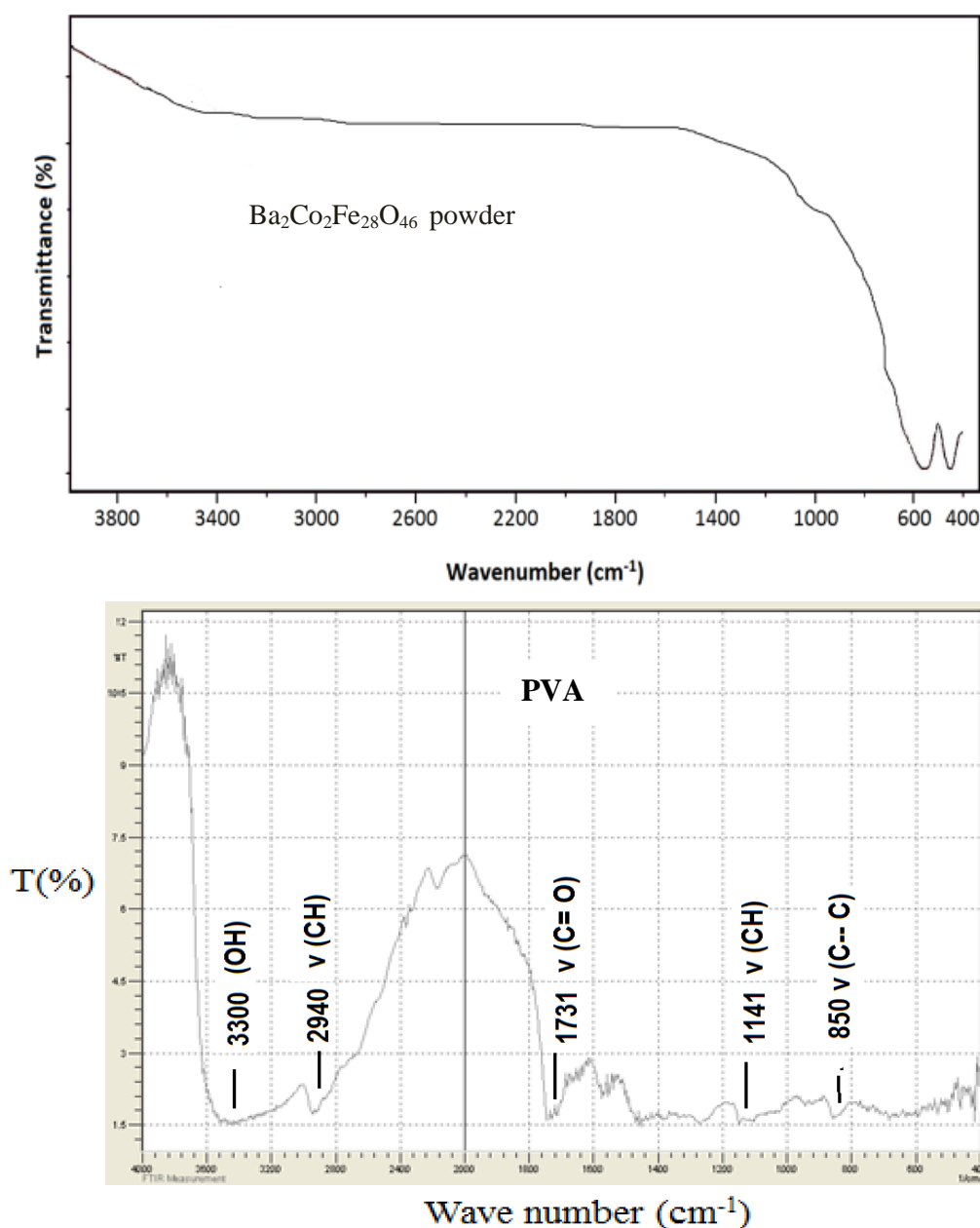
Fig. 2: *FTIR spectra of Ba₂Co₂Fe₂₈O₄₆ hexaferrite powder, PVA and composite samples with different mass ratio of ferrite to PVA.*

Figure 2 shows FTIR spectra of calcined $Ba_2Co_2Fe_{28}O_{46}$ powder, PVA and composites with different mass ratio of ferrite to PVA (9:1, 8:2, 7:3, 6:4 and 5:5). The broad band observed in PVA sample at 3,300 cm^{-1} may be assigned to O–H stretching due the strong hydrogen bond, the absorption bands around 2940 cm^{-1}, 1141 cm^{-1} are the C–H alkyl stretching bands. The absorption band at approximately 1,731cm^{-1} may be attributed to the stretching vibration of νC=O and the band observed at 850cm^{-1} may be assigned to C–C

stretching [20–22]. The existence of weak absorption bands in $Ba_2Co_2Fe_{28}O_{46}$ powder sample between 400 cm^{-1} to 700 cm-1 are due to stretching of M-O, which attributed to the formation of the ferrite phase [23, 24]. Composite samples show all absorption bands of PVA as well as weak band of ferrite at 440 cm^{-1}.

XRD Analysis
XRD measurements were carried out at room temperature on an X-ray diffracto-meter model

_____

no. Make – seifert; XRD 3000 PTS with scanning rate of 0.08^o /min using CuK_α radiation (λ = 1.5406 Å). XRD patterns of PVA, $Ba_2Co_2Fe_{28}O_{46}$ and $Ba_2Co_2Fe_{28}O_{46}$ hexaferrite-PVA composite samples for the different mass ratio 9:1, 8:2, 7:3, 6:4 and 5:5 are shown in Figures (3a-b) respectively. The strong crystalline reflections observed in the X-ray diffraction pattern of PVA (shown in Figure 3a) at 2θ = 19.88° and 20.18° (d = 4.46 and 4.39, respectively), which are characteristic of PVA [25]. The diffused peaks at higher angles confirm the semi-crystalline nature of the polymer. The XRD patterns of $Ba_2Co_2Fe_{28}O_{46}$ hexaferrite powder and composite samples were indexed with the standard patterns for X-type hexagonal crystals. The nature of XRD patterns shows the formation of mono phase. All the diffraction peaks were indexed in agreement with the reported hexagonal crystal structure [3]. It is clear from Figure 3b that there is no separate peak of PVA may be due to appearance of similar peak of hexaferrite at around 40° hence difficult to detect. Lattice parameters and cell volume of $Ba_2Co_2Fe_{28}O_{46}$ hexaferrite and ferrite-PVA composites are listed in Table 2. There is no any change of lattice parameters and cell volume with increasing concentration of PVA.
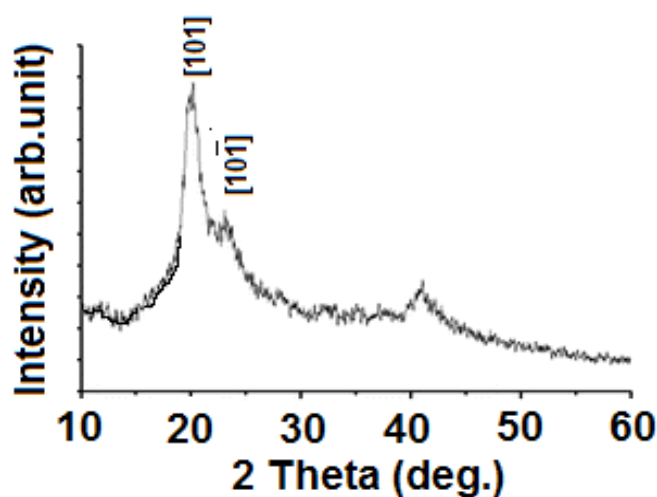

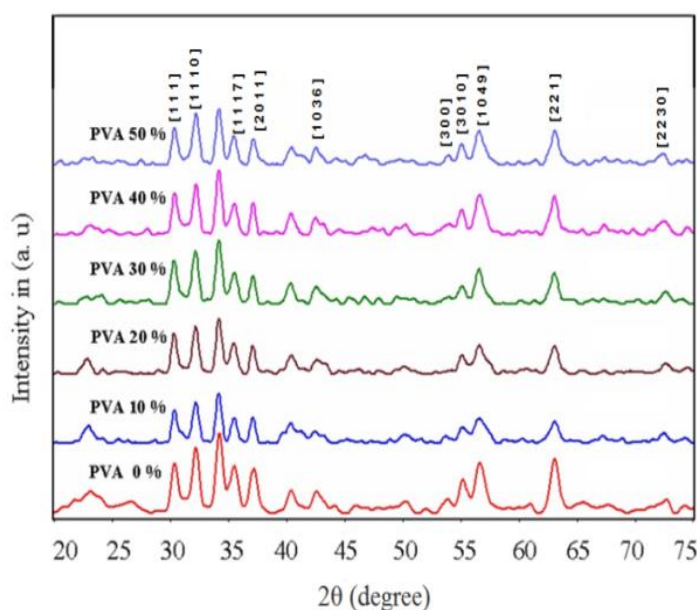
Fig. 3a: *X-ray diffraction pattern of PVA [25].*

Fig. 3b: *XRD patterns of $Ba_2Co_2Fe_{28}O_{46}$ and $Ba_2Co_2Fe_{28}O_{46}$ hexaferrite - PVA composites with different mass ratio 9:1, 8:2, 7:3, 6:4 and 5:5.*

_____

Table 2: Lattice parameters and cell volume of X-type BaMe$_2$Fe$_{28}$O$_{46}$ hexaferrite- PVA composites.

Sr.No.	Ba$_2$Co$_2$Fe$_{28}$O$_{46}$ – PVA mass ratio	Peak	Lattice parameters a (Å) c (Å)		Cell volume V (Å)^3
1	10:0	1 1 1 0	5.880	84.3	6182.78
2	9:1	1 1 1 0	5.891	84.3	6205.94
3	8:2	1 1 1 0	5.895	84.1	6199.62
4	7:3	1 1 1 0	5.895	84.1	6199.62
5	6:4	1 1 1 0	5.89	84.3	6203.84
6	5:5	1 1 1 0	5.89	84.1	6189.17

SEM Analysis

Microstructures of prepared Ba$_2$Co$_2$Fe$_{28}$O$_{46}$ powder and polymer composites samples were studied using a scanning electron microscopy. The SEM images prepared Ba$_2$Co$_2$Fe$_{28}$O$_{46}$ powder sample and hexaferrite-PVA composites are shown in Figure 3. It is evident from Figure 4a that majority grains are non-uniform and forms clusters. The grain size is found to be in the range of 200-300 nm. the

SEM images of composite samples show that distribution of powders of barium cobalt ferrite in polymer matrix is irregular and porosity decrease with incresing of PVA concentration. One conclude from morphology study that distribution of powders of barium cobalt hexaferrite in polymer matrix is irregular and powder particles are of irregular shapes and different sizes.
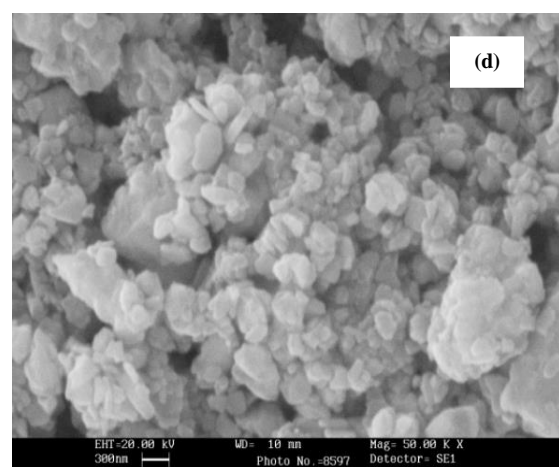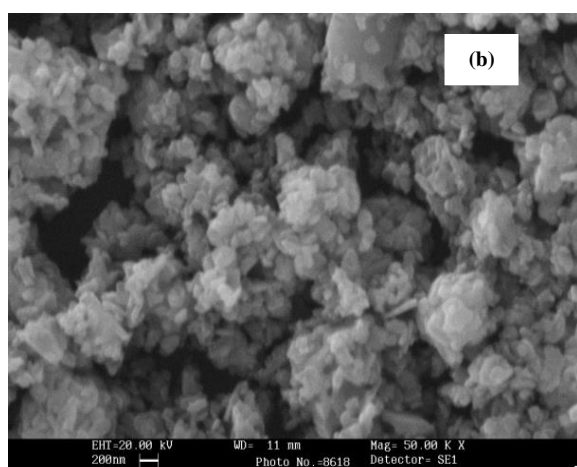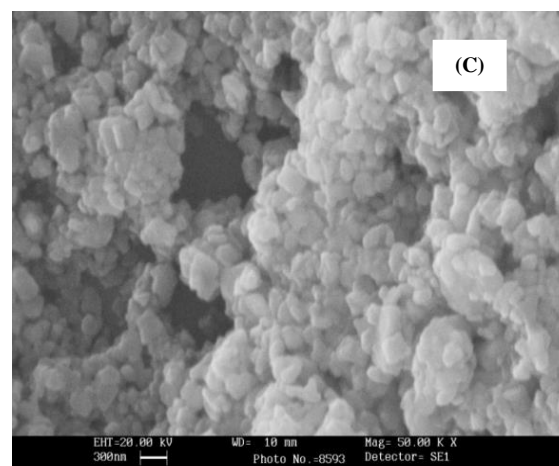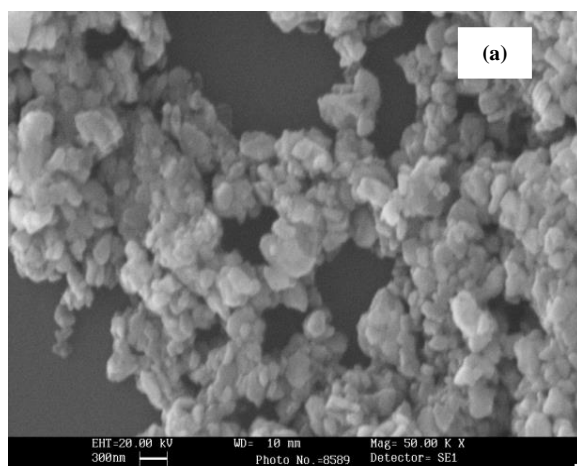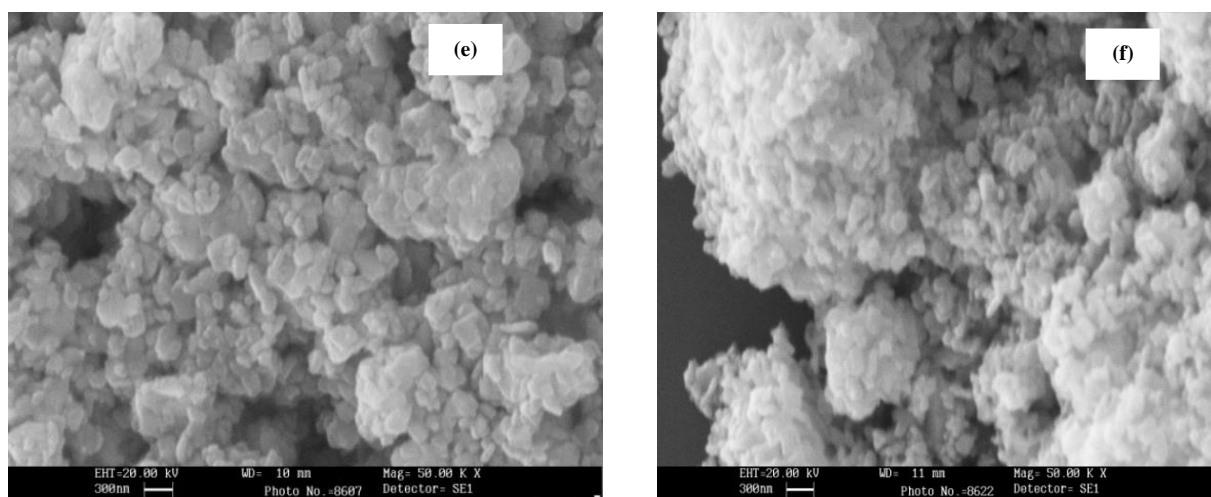
Fig. 4: *SEM Micrographs of (a) $Ba_2Co_2Fe_{28}O_{46}$ powder (b-f) $Ba_2Co_2Fe_{28}O_{46}$-PVA Composites for the Mass Ratio 9:1, 8:2, 7:3, 6:4, 5:5, Respectively.*

Dielectric Properties

The dielectric measurements were carried out over the frequency range of 200 Hz to 2 MHz at room temperature using an Agilent Precision LCR meter (Model No. E4980A). Dielectric loss tangent (tan δ) of all the samples was calculated using equation (1)

$$\boldsymbol{tan\ \delta} = \frac{\varepsilon'}{\varepsilon''} \tag{1}$$

Where ε' is a real dielectric constant and ε'' is a complex dielectric constant. The variation of dielectric constant (real ε') and dielectic loss tangent (tan δ) as a function of frequency for composte samples with different mass ratio of PVA (from 9:1, 8:2, 7:3, 6:4 and 5:5) are shown in Figures 5 (a) and (b), respectively.
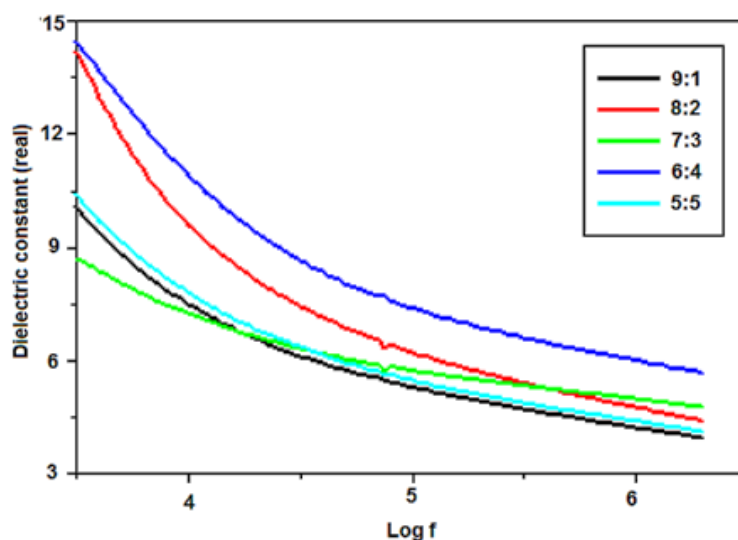

Fig. 5a: *The Variation of Dielectric Constant (real) with Log Frequency of $Ba_2Co_2Fe_{28}O_{46}$ -PVA Composite Samples with Different Mass Ratio.*

It is clear from Figures 4a, b that the value of dielectric constant (as well as dielectric loss tangent) decreases with increasing of frequency for all the samples. The variation of dielectric constant with frequency reveals the dispersion due to Maxwell-Wagner [26, 27] type interfacial polarization in agreement with

Koop's phenomenological theory [28]. The dielectric properties of polycrystalline ferrite-polymer composites are depend upon two factors: the interfacial polarization and intrinsic electric dipole polarization. Interfacial polarization results from the heterogeneous structure of ferrites comprising low-

_____

conductivity grains separated by higher resistivity grain boundaries [28]. These grain boundary layers may be attributed to the superficial reduction or oxidation of the crystals in the porous material as a result of their direct contact with the firing atmosphere. The higher value ε', for composite with mass ratio 6:4 may be due to the significant contribution of Co^{2+} ions in addition to Fe^{3+} and Fe^{2+} ions to interfacial polarization. The dielectric loss tangent represents the phase lag of the dipole oscillations with respect to the applied electric field, depends on the number and nature of ions present.
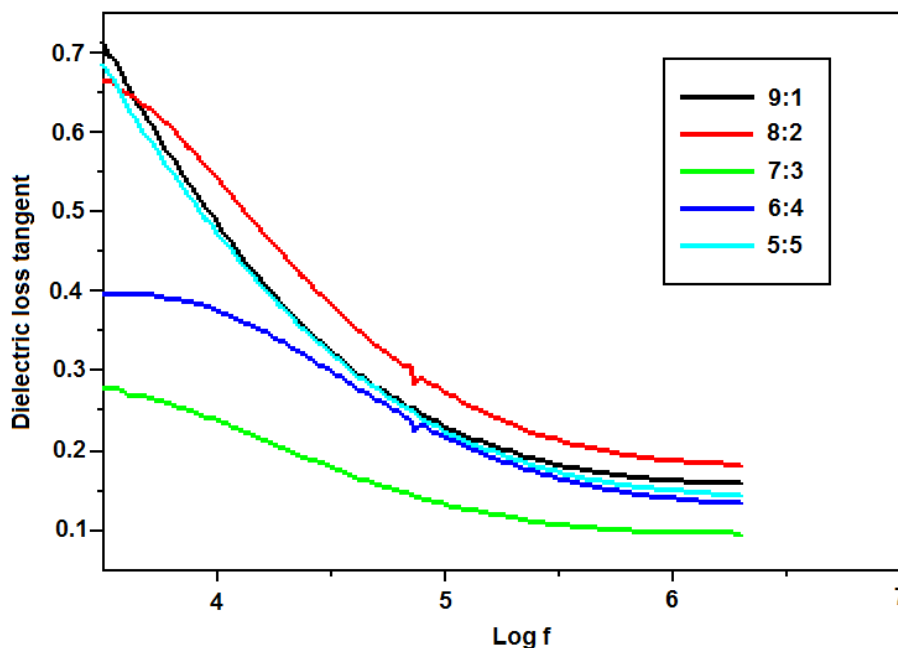

Fig. 5b: *The Variation of Dielectric Loss Tangent (tan δ) with Log Frequency of $Ba_2Co_2Fe_{28}O_{46}$ - PVA Composite Samples for Different Mass Ratio.*

CONCLUSION
X-type $Ba_2Co_2Fe_{28}O_4$ powders were successfully synthesized using a reverse co precipitation technique. $Ba_2Co_2Fe_{28}O_4$-PVA composites were prepared with different mass ratio. Structural as well as dielectric properties of $Ba_2Co_2Fe_{28}O_4$-PVA composites studied at room temperature. The observation from XRD, SEM, and FTIR can be summarized as follows.

(1) FTIR result confirms the formation of ferrite.
(2) The X-ray diffraction investigations confirm the formation of mono-phase of hexaferrite.
(3) Scanning electron microscopy images reveal that the shape and size of formed barium cobalt hexaferrite powder particles is non-uniform. The particle size is in the order of 200–300 nm. The addition of PVA does not changed the shape and size of particles but porosity decreased.

REFERENCES
1. Pullar R. C. *Progress in Materials Science* 2012; 57 (7): 1191p.
2. Smit J. and Wijn. H.P.J. *"Ferrites", Eindhovan, Philips Technical Library.* 1959
3. Braun P. B. *Philips Res. Rep.* 1957; 12: 491p.
4. Ladislav Valko et al. *Journal of Electrical Engineering* 2003; 54(3–4): 100p.

_____

5. Stabik J. et al. *Archives of Material science and Engineering* 2010; 41(1):13p.
6. Yahya N. et. al. *International Journal of Basic & Applied Sciences* 2009; 09: 30p.
7. B. X. Gu, *J. Appl. Phys.* 1991; 70: 372p.
8. B. X. Gu, *J. Appl. Phys.* 1992; 71: 5103p.
9. B. X. Gu, *J. Appl. Phys.* 1994; 75:4114p.
10. Xiong G.and Mai Z.H., *J Appl Phys* 2000; 88(1): 519–523p.
11. Pullar R. C. and Bhattacharya A. K. *J. Mater. Sci.* 2001; 36: 4805p.
12. Haijun Z., Xi Y., and Liangying Z., *J. Magn. Magn. Mater.* 2002; 241: 441p.
13. Haijun Z., Zhichao L., Xi Y., et al. *Mater. Res. Bull*. 2003; 38: 363p.
14. Kenji Kamishima, Nobuyuki Hosaka, Koichi Kakizaki, et al. *Journal of Applied Physics* 109. (2011). 013904p. doi: 10.1063/1.3527933
15. Langhof, Seifert D., Göbbels M., et al. *J. Solid State Chem*. 2009; 182: 2409p.
16. Garrel D.R., *The Journal of surgical research*, 51, (1991) 297–302p.
17. Kim J.H. et al. *Journal of Applied Polymer Science*, 45, 1992.1711–1717.
18. Saxena A K *Tissue Engineering*, 5, 1999525–532p.
19. Peppas N.P. *Journal of Biomedical Materials Research*, 11, 1977,423–434p.
20. Mansur H.S. et al. *Polymer* 2004. 45.7193p.
21. Andrade G. et al. *Biomed Mater* 2006.1.221p.
22. Mansur H.S. et al. *J Mater Sci: Mater Med* 2005.16.333p.
23. Song F., Shen X., Xiang J., Song H., *Mater. Chem. Phys*. 2010; 120: 213p.
24. Ashiq M. N., Iqbal M. J., Gul I. H, *J. Alloys Compd* 2009; 487: 341p.
25. Siddhi Gupta et al. *J Mater Sci: Mater Med* 2011; 22: 1763p.
26. Maxwell JC, Electricity and Magnetism, vol. l, Oxford Univ. Press, New York, 1973.
27. K.W. Wagner, *Amer. Phis.* 1973; 40: 817p.
28. C.G. Koops, *Phys. Rev.* 1951; 83: 121p.